Elastic anisotropy and extreme Poisson's ratios in single crystals

Zoe A.D. Lethbridge [a], Richard I. Walton [a,*], Arnaud S.H. Marmier [b],
Christopher W. Smith [b], Kenneth E. Evans [b]

[a] *Department of Chemistry, University of Warwick, Gibbet Hill Road, Coventry CV4 7AL, UK*
[b] *Engineering Mathematics and Physical Sciences, Harrison Building, University of Exeter, North Park Road, Exeter EX4 4QF, UK*

Abstract

The relationship between elastic anisotropy and extreme Poisson's ratio behaviour (either positive or negative) in single-crystalline materials has been investigated using experimentally determined single-crystal elastic constants for a wide range of solid materials. This makes use of a recently proposed elastic anisotropy index that is applicable to all crystal symmetries. For many real materials we find a striking correlation between the value of the elastic anisotropy index and the magnitudes of maximum and minimum Poisson's ratios and this is independent of crystal symmetry. This structure–property relationship provides new examples of auxetics and shows that negative Poisson's ratios are actually not uncommon among many classes of inorganic (and organic) materials, including elemental metals, alloys, ionic solids, molecular solids and giant covalent networks.

1. Introduction

A negative Poisson's ratio in a solid defines the counter-intuitive lateral widening upon application of a longitudinal tensile strain. The phenomenon, also described as auxetic behaviour [1], has a wide range of potential technological applications such as indentation resistant materials, improved honeycomb dielectrics, self-adaptive vibration damping materials, molecular membranes and actuators or sensors for MEMS applications, shear resistant materials, improved sound and shock absorption, naturally simplistically curved (dome-shaped) surfaces, and medical applications such as artery dilators. The progress in the study of auxetics for these practical uses has been the subject of several review articles [2–5]. The first synthetic auxetic materials were foams and microporous polymers, where structure on the microscopic scale was fabricated to give so-called, re-entrant geometries that underwent lateral expansion upon stress [6,7]. A few crystalline solids have also been reported as having negative Poisson's ratios on the basis of their experimentally measured elastic stiffness matrices from single crystals, including certain elemental metals [8], the silica polymorph α-cristobalite [9], the oxide paratellurite, α-TeO$_2$ [10], and the zeolite mineral natrolite [11]. For some of these materials, attempts have been made to relate negative Poisson's ratios to atomic-scale structure by visualizing crystal structures as being made up of rigid building units linked by flexible hinges [11–13], akin to the models used to explain the behaviour of auxetic polymers. For the elemental metals a specific mechanism, based on the interactions between hard spheres in specific crystal planes that give rise to auxetic behaviour, was proposed [8].

It is noteworthy that although there are many published reports of experimental measurements of single-crystal elastic constants of a variety of materials [14], there are actually relatively few quoted examples of materials with negative Poisson's ratios. In looking for a more detailed understanding of the origin of negative Poisson's ratios in

* Corresponding author.
  E-mail address: r.i.walton@warwick.ac.uk (R.I. Walton).

solid-state materials, it is important to provide new examples of crystalline materials that show the phenomenon. So far single-crystalline materials that possess negative Poisson's ratios have been treated as unusual, and therefore knowledge of new materials with the property would be helpful to the understanding of structure–property relationships, since crystallography also provides details of the atomic-scale structure of such materials. A number of authors have described mathematical descriptions of the theoretical limits on Poisson's ratio (both positive and negative) for single-crystalline materials and how they depend on crystal symmetry: indeed, the physically allowable extreme ranges of the possible values of Poisson's ratios, for all possible crystal symmetries, have been extensively examined theoretically [15–24] Although it might be expected that elastic anisotropy has no relationship to the symmetry of the crystal being considered, in general the property has been analysed by treating each crystal symmetry individually.

The Poisson's ratio, v_{ij}, for any material is most simply described as a ratio of compliance coefficients:

$$v_{ij} = -\frac{S_{ij}}{S_{ii}} \qquad (1)$$

where S_{ij} are tensorially rotated elements of the compliance matrix. The expressions for Poisson's ratios in non-axial directions as functions of non-rotated compliance coefficients are more complex, but can be obtained by transformation and also defined in terms of stiffness coefficients, C_{ij}; this is documented in standard texts [25]. The Poisson's ratios on the principal axes of a material are limited by a simple ratio of Young's moduli, E [15]:

$$v_{ij} < (E_i/E_j)^{1/2} \qquad (2)$$

Ting and Chen [19], Boulanger and Hayes [16], Norris [21] and Rovati [17,18] have explored the allowable range of values of Poisson's ratios for various different symmetries. However, whilst these works explore the range of values that are feasible, based on physically allowable elastic constants and the three-dimensional variation of these constants as a function of the direction cosines, they do not examine systematically the experimentally measured values, or the physical causes, such as the underlying atomic-scale crystal structure for the values that are found experimentally.

The elastic properties of single crystals are described using a tensor notation that makes a direct comparison between materials that have related chemical structures but different symmetry less than straightforward. A simple means of classifying the elastic properties of single crystals is to consider elastic anisotropy; indeed it is intuitively expected that materials with a high degree of elastic anisotropy may show the most extreme elastic behaviour, with large maximum and minimum values of, for example, Poisson's ratios. The Zener ratio, Z, is perhaps the best known measure of the anisotropy of elastic behaviour, and this applies for cubic single crystals, and was introduced in 1947 in a study of β-brass [26]. The ratio of the two shear coefficients it is given by (using the conventional Voigt matrix notation of the c_{ij} elements of the stiffness matrix):

$$Z = \frac{2c_{44}}{c_{11} - c_{12}} \qquad (3)$$

$Z = 1$ then is defined to indicate elastic isotropy, i.e., when $c_{44} = (c_{11} - c_{12})/2$.

Since the time that the Zener ratio was proposed for cubic materials, a wide variety of elastic anisotropy measures have been reported in the literature. These use either various combinations of single-crystal elastic constants and are usually presented for cubic materials but occasionally for lower symmetries [27–30] or as ratios of experimentally measured compression or shear velocities of acoustic phonons [31].

In addition to numerical indicators of anisotropy, the variation of elastic moduli with direction is also of relevance. In 1971, Turley and Sines examined E, G, and v values in specific planes in the cubic system using direction cosines [32]. Li et al. examined hexagonal [33], trigonal [33] and tetragonal [34] symmetries, giving expressions for examining the behaviour of Young's modulus, shear modulus and Poisson's ratio with variation of direction using the Euler angles. They studied cadmium and thallium [34], and found a negative Poisson's ratio in cadmium which they observed was structurally more anisotropic than thallium (a higher c/a ratio).

Ledbetter and Migliori recently proposed a way of calculating an anisotropy ratio, related to the Zener ratio, that can be applied to all crystal systems, i.e., is independent of crystal symmetry [35]. They invoked Christoffel's equation to derive an expression for anisotropy (A^*) as a ratio of maximum and minimum shear sound wave velocities, as measured in scattering or ultrasound experiments, over all propagation and polarisation directions.

$$A^* = \frac{v_{max}^2}{v_{min}^2} \qquad (4)$$

Here $A^* = 1$ represents isotropy. Note that from this definition, $A^* \geqslant 1$. Although some cubic materials have $Z < 1$, this equates to a value of $1/A^*$. More recently Ranganathan and Ostoja-Starzewski proposed a "Universal Elastic Anisotropy Index", A^U, which is simply related to various definitions of aggregate moduli [36]:

$$A^U = 5\frac{G^V}{G^R} + \frac{K^V}{K^R} - 6 \qquad (5)$$

G and K are shear and bulk moduli, respectively, and the superscripts V and R denote Voigt and Reuss averages, respectively. In this case $A^U = 0$ defines isotropy. In practice this index has little advantage over the one proposed by Ledbetter and Migliori for experimentally determined elastic constants, since in practice it requires knowledge of both c_{ij} and s_{ij} values to implement, rather than sound velocities that would be measured in experiment (see Supporting Information for a comparison of A^* and A^U for the materials that we consider below).

In this paper we survey a range of published experimental elastic constants, using the Ledbetter and Migliori elastic anisotropy ratio to classify extreme Poisson's ratio in a large number of single crystals that include examples of all crystal symmetries. Our aim was to uncover new examples of materials that show extreme elastic behaviour, and then to examine whether a simple relationship, applicable to all crystal symmetries, exists between elastic anisotropy and the occurrence of negative Poisson's ratios on the basis of their experimentally reported elastic constants.

2. Methodology

In order to use the concept of elastic anisotropy to explore Poisson's ratio behaviour in real materials we investigated the application of the Ledbetter and Migliori ratio, A^* [35]. We have concentrated on studying materials for which elastic constants have been measured experimentally and are available in the literature, either tabulated in the Landolt–Börnstein tables [14], or taken directly from more recently published reports. This includes values that have been determined using resonant ultrasound spectroscopy, laser Brillouin spectroscopy and inelastic X-ray and neutron scattering. From the literature we selected 472 sets of elastic constants (usually different materials but in some cases a single material whose elastic constants had been measured at more than one temperature, or by more than one group of researchers), the full details of which are tabulated in supplementary information. The examples cover all triclinic, orthorhombic and hexagonal materials tabulated in the Landolt–Börnstein tables, and a representative number of monoclinic, tetragonal, trigonal and cubic materials.

Maximum and minimum values of Poisson's ratio, their directions, and values of A^* were evaluated using the program ElAM (http://hdl.handle.net/10036/77859) [37]. This program allows the calculation and visualization of three-dimensional elastic properties of single-crystalline materials with knowledge of elastic constants. The ElAM code carries out the tensorial operations needed to calculate the values of elastic properties in any given direction upon input of the elements of the stiffness matrix, c_{ij}. Most properties (Young's and shear modulus, compressibility, Poisson's ratio) only require tensorial inversion and rotation, but the determination of wave velocities (necessary to calculate A^*) also calls for the diagonalization of the dynamic matrix. In its standard mode, ElAM scans the unit sphere to create 3D models of an elastic property's anisotropy. This 3D representation can be explored easily on screen within ElAM to allow easy identification of any unusual elastic properties. It can also produce 2D cuts in any given plane and compute averages following various schemes (Reuss, Voigt, Hill, direct). More importantly for this study, it can also query a database of elastic constants for properties (minima, maxima, averages), and associated significant directions (for instance the direction in which a Poisson's ratio is minimum or maximum).

3. Results and discussion

Maximum and minimum Poisson's ratios were calculated as two separate datasets from c_{ij} values for 113 cubic materials and are plotted against anisotropy, $A^*(=Z$ in this case) in Fig. 1a. The extreme Poisson's ratios all lie along two curves, which appear approximately symmetrical with a single point of intersection. The apparent trends have no relationship to the chemical nature of the material (see Supporting Information). For example, in addition to the solids mentioned in Section 1, materials that possess negative Poisson's ratios in some crystallographic direction include the transition-metal oxide ReO_3; the molecular solid iodine; the mineral anhydrite, $CaSO_4$, a simple inorganic salt; the infinite chain structure of trigonal, elemental selenium; and the organic, molecular solids triphenylbenzene and urea, Table 1. To the best of our knowledge these materials have never been specifically reported as possessing negative Poisson's ratios: the advantage of using the Elam program is an easy exploration of all crystallographic directions to interrogate efficiently the elastic properties of a wide range of materials. Fig. 1b shows similar plots of maximum and minimum Poisson's ratio against A^* that includes materials of lower
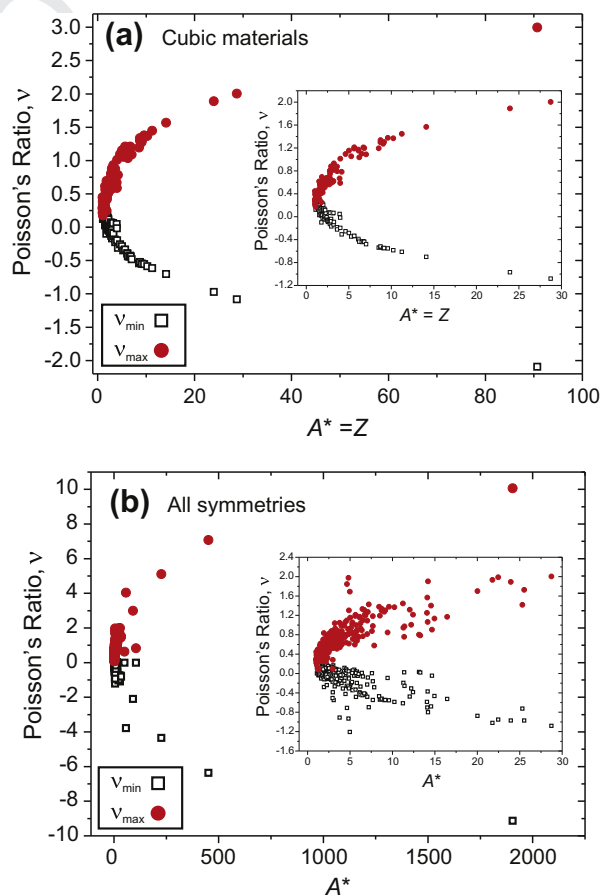

Fig. 1. Plots of maximum and minimum Poisson's ratio against elastic anisotropy. (a) For cubic materials using the Zener ratio, $Z (=A^*)$, and (b) for all crystal systems using the Ledbetter and Migliori elastic anisotropy index A^*. In both plots the insets are expanded regions of the main graphs.

Table 1
Examples of materials possessing negative Poisson's ratios in some crystallographic direction, listed in order of increasing elastic aniosotropy (A^*). The directions of maximum and minimum Poisson's ratios, v_{min} and v_{max} respectively, are expressed for convenience using the Miller system [h k l] with the load and transverse directions quoted for each extreme Poisson's ratio. Note that the use of the Miller system is not exact and the program ElAM also provides a unit vector description of the directions of extreme Poisson's ratios. The reference is to the source of single-crystal elastic constants.

Material	Crystal system	A^*	v_{min}	Load direction (v_{min})	Transverse direction (v_{min})	v_{max} Load direction (v_{max})	Transverse direction (v_{max})	Reference
Natrolite $Na_2Al_2Si_3O_{10} \cdot 2H_2O$	Orthorhombic	2.27	−0.12	[−1 1 0]	[1 1 0]	0.46 [−3 3 5]	[22 −21 26]	[51]
α-Quartz (SiO_2)	Trigonal	2.29	−0.09	[0 27 29]	[1 0 0]	0.31 [0 −23 33]	[1 0 0]	[52]
Ag	Cubic	2.92	−0.08	[1 0 1]	[1 0 −1]	0.81 [1 0 1]	[0 1 0]	[14]
α-Cristobalite (SiO_2)	Tetragonal	2.94	−0.51	[7 7 9]	[−19 −19 30]	0.10 [1 1 0]	[−1 1 0]	[9]
ReO_3	Cubic	3.98	−0.01	[0 0 1]	[26 −31 0]	0.59 [1 0 1]	[10 −1]	[14]
$CaSO_4$	Orthorhombic	5.91	−0.05	[−9 10 −15]	[−7 7 9]	0.76 [−24 30 −11]	[15 13 1]	[14]
Triphenylbenzene	Orthorhombic	6.52	−0.06	[11 29 −25]	[14 −27 −25]	0.77 [8 −13 13]	[341 −21]	[14]
Selenium	Trigonal	7.12	−0.08	[25 11 −29]	[−13 14 −6]	1.27 [0 −6 19]	[1 0 0]	[14]
Iodine	Orthorhombic	12.34	−0.48	[0 1 0]	[0 0 1]	1.32 [0 0 1]	[1 0 0]	[14]
AuCd	Cubic	14.10	−0.70	[9 9 4]	[−1 1 0]	1.57 [7 7 −2]	[2 2 13]	[14]
Urea	Tetragonal	14.22	−0.80	[−16 −16 33]	[12 12 11]	1.91 [−2 −2 5]	[−1 1 0]	[14]
α-TeO_2 (paratellurite)	Tetragonal	32.73	−0.75	[10 0 17]	[17 0 −10]	1.45 [2 0 3]	[0 1 0]	[40]
CsH_2PO_4	Monoclinic	53.46	−1.93	[−10 17 −4]	[35 20 −4]	2.71 [10 −33 21]	[39 11 −1]	[14]

symmetries (472 in total), also calculated using ElAM. The same general shape of the two curves is observed, and they intersect at $A^* = 1$: for example, A^* is very close to 1 for elemental tungsten, with $v_{max} = v_{min} = 0.280$, and for nickel silicate, Na_2SiO_4, $A^* = 1.005$, $v_{max} = 0.298$ and $v_{min} = 0.295$. Our analysis shows that there is no relationship between crystal symmetry and the distribution of points in Fig. 1b, nor is there any relationship, applicable to all crystal systems, between the directions at which the extreme values of Poisson's ratios are observed (see Supporting Information for tables of the materials we have studied and the analysis of their elastic constants). This implies that it is the crystal structures of the materials that are responsible for the shapes of the curves, i.e., the nature of constituent interatomic forces and their relative directions with respect to each other, and not an artefact arising from the conventional symmetry descriptions of their structures.

An important observation from the two plots in Fig. 1 is that negative Poisson's ratios occur in many materials and in fact from these experimentally derived points all real cubic materials with $A^* > 4$ show a negative Poisson's ratio in some combination of crystal load direction and transverse plane. Previous work on the theoretical limits of Poisson's ratios of cubic materials, such as that by Paszkiewicz and Wolski, would predict that all materials with Z ($=A^*$) > 3 should have a negative Poisson's ratio [24], consistent with the experimental data we have analysed. It is worth noting that errors on measured c_{ij} values have rarely been quoted in the literature; the origin of the scatter of the experimental data points in Fig. 1 should also be considered. For lower symmetries, where a greater number of stiffness constants must be determined, it is probable that some greater experimental error is present since a greater number of independent experimental measurements is needed, and this might explain the greater scatter of the points in Fig. 1b. A feel for the error in Poisson's ratios

may be gained by looking at materials for which several sets of experimentally reported elastic constants are reported and that have been measured independently by different groups. For example, for tetragonal paratellurite (α-TeO_2) at least four sets of elastic constants are available [38–41], and our analysis of these gives minimum Poisson's ratios ranging from −0.73 to −0.8 and maximum Poisson's ratios ranging from 1.42 to 1.52 (Supporting Information). This would explain some of the scatter seen in the analysis we have presented in Fig. 1.

It is initially worth considering some of the outlying points which do not conform to the general curves seen in Fig. 1, and for these we can identify two distinct classes of material. There is first the case of layered materials, Table 2. Graphite and boron nitride are both constructed from covalently bonded layers with weak inter-layer van der Waals forces and are classical examples of highly anisotropic crystal structures. They also both have rather large values of A^*: 110 and 52, respectively, reflecting the high degree of anisotropy also in their elastic constants. The Young's modulus in the plane of the layers is large (graphite 1092 GPa, boron nitride 776 GPa), while perpendicular to the layers it is much smaller (graphite 39 GPa, boron nitride 27 GPa). A zero Poisson's ratio is the minimum observed and this corresponds to a force applied perpendicular to the layer, where the physical effect of changing the inter-layer spacing but not the interatomic separations within the layers would be observed, Fig. 2. Molybdenum disulfide is another example of a layered material whose elastic constants have been reported (from X-ray and neutron scattering data) [42]: the anisotropy here is lower ($A^* = 7.68$) compared to the cases of graphite and boron nitride, possibly reflecting a greater bonding interaction between the sulfide layers, but maximum and minimum values of Young's modulus and Poisson's ratio are 210 GPa and 46 GPa, and 0.57 and −0.28, respectively. The extreme values of Poisson's ratio for ele-

Table 2

Examples of layered materials that show anomalous Poisson's ratio behaviour owing to their highly anisotropic atomic-scale structures. Legend is as for Table 1.

| Material	Crystal system	A^*	v_{min}	Load direction (v_{min})	Transverse direction (v_{min})	v_{max}	Load direction (v_{max})	Transverse direction (v_{max})	Reference
Arsenic	Trigonal	4.81	−0.93	[0 37 14]	[1 0 0]	1.98	[0 19 6]	[0 −6 19]	[14]
MoS_2	Hexagonal	7.85	−0.28	[25 32 0]	[−32 25 0]	0.58	[−2 3 0]	[0 0 1]	[14]
Boron nitride	Hexagonal	51.53	0.00	[0 0 1]	[−40 1 0]	0.64	[10 35 16]	[4 15 −37]	[53]
Graphite	Hexagonal	107.94	0.00	[0 0 1]	[−40 1 0]	0.83	[22 29 16]	[10 13 −37]	[14]
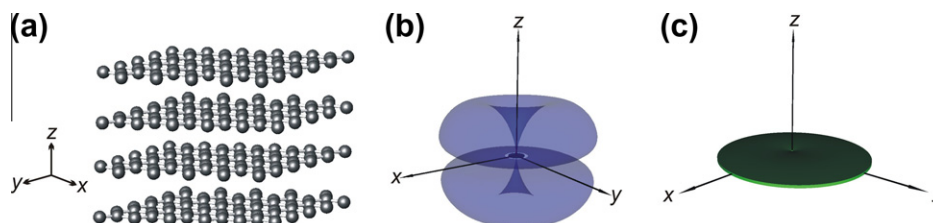
Fig. 2. Example of the anisotropic elasticity of a layered material. Here, the case of graphite, whose structure (hexagonal rhombohedral symmetry) is shown in (a), shows a zero Poisson's ratio along Z, as illustrated by the three-dimensional surface representation of the Poisson's ratio shown in (b) and correspondingly anisotropic Young's moduli as shown in (c).
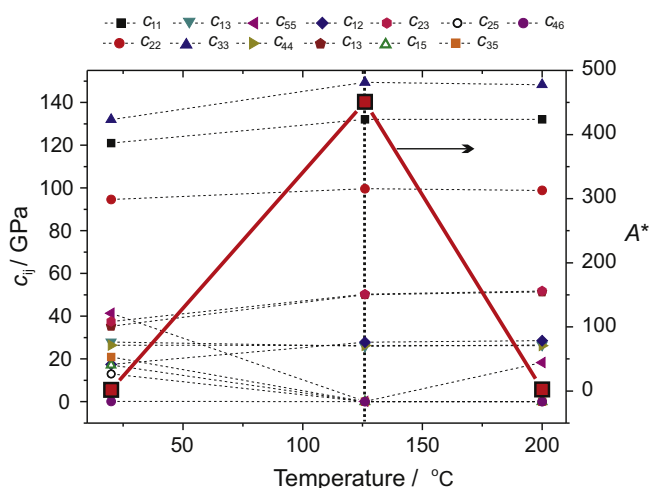

Fig. 3. Example of a highly anisotropic elasticity of a material close to a structural phase transition. The case of LaP_5O_{14} is shown where c_{ij} values of the materials at three temperatures are plotted along with values of A^* (denoted by the large red squares). Data were taken from Ref. [44] and the temperature of phase transition (126 °C) is shown by the vertical dotted line. (For interpretation of the references to colour in this figure legend, the reader is referred to the web version of this article.)

mental arsenic also lie some distance away from the typical curves in Fig. 1: there are two reported sets of elastic constants that give $A^* = 4.815$ and $A^* = 4.640$ with minimum Poisson's ratios of −0.709 and −0.93, respectively. The arsenic structure consists of double layers with weak inter-layer bonding, and as with graphite and boron nitride, the anisotropy of the structure is reflected in its unusual elastic properties [43].

The second class of "outlying materials" on Fig. 1 are those whose elastic constants have been measured at a temperature and pressure close to a structural phase transition. Aside from the layered materials described above, all mate-rials with $A^* > 35$ in our survey fall into this category. Carpenter and Salje have already surveyed the use of Landau theory to predict how elastic constants vary with different classes of phase change [44]: as certain transitions are approached, the velocity of certain acoustic phonons can tend to zero (soft acoustic modes), thus associated elastic constants (or symmetry adapted combinations) may also decrease to zero. This behaviour can then lead to a large elastic anisotropy, which in turn can give some extreme values of Poisson's ratios. Lanthanum pentaphosphate, LaP_5O_{14}, is a clear example of this: it is monoclinic below 126 °C and becomes orthorhombic above this temperature [45]. Its A^* value shows a dramatic increase at the phase transition to a value of 451, falling back to 2.4 at 200 °C; at the phase tran-sition the maximum and minimum Poisson's ratios are 7.01 and −6.36, respectively. This behaviour is plotted in Fig. 3. For InTl alloys with a range of compositions a softening of certain phonon modes is observed near a cubic-tetragonal phase change [46]; indeed elastic constants from $In_{0.73}Tl_{0.27}$ at 125 K (the transition temperature) show $A^* = 1904$, with maximum and minimum Poisson's ratio of 1.996 and −0.997, respectively [47]. The In−Tl alloys have been well studied in the literature because of this extreme anisotropy: in the case of the 27% Tl analogue the phase transition is a martensitic face-centred tetragonal to face-centred cubic transition where $1/2(C_{11} − C_{12})$ approaches zero at the tran-sition [48]. For martensitic phase transformations, it is well established that they may be accompanied by a lattice soften-ing and a large elastic anisotropy [49]. Other examples of this behaviour include the molecular material betaine maleate, $[(CH_3)_3NCH_2COOH][(COOH)(CH_2)(COO)]$, for which a large increase in anisotropy is seen at a low temperature phase transition [50], and sodium azide, which undergoes a ferroelectric transition on cooling at 20 °C from a trigonal to monoclinic and for which room temperature elastic

measurements show a high A^* value of 226, with an associated minimum Poisson's ratio of -4.35 [51].

Aside from these "outlying cases", previous theoretical work on the extremal values of Poisson's ratio does not explain why so many different solids follow the apparently simple behaviour shown by Fig. 1, and why the behaviour is independent of crystal symmetry. Baughman et al. provided some insight into the possible cause of this extremal behaviour in the specific case of elemental metals and their alloys, by considering cubic symmetry and suggesting that the atoms be treated as hard spheres [8]. We here adopt a more general approach to the interaction of spheres, based on that found in the literature concerning granular solids [52,53]. This model assumes that neighbouring spheres have two interaction constants, a normal force constant, k_n and a tangential force constant k_t. The interaction between spheres can then be specified by:

$$\lambda_1 = k_t/k_n \tag{6}$$

So, hard spheres have $\lambda_1 \to 0$ and spheres dominated by a tangential interaction have $\lambda_1 \to \infty$. Assuming a random distribution of spheres and averaging over the ensemble, Bathurst and Rothenburg [52,53] showed that:

$$v = (1 - \lambda_1)/(4 + \lambda_1) \tag{7}$$

Since it is apparent that λ_1 may itself be considered a measure of anisotropy in bonding, we have also made the assumption that a linear relationship exists between λ_1 and A^*: in fact we find by defining the relationship $\lambda_1 = A^* - 1$ an excellent agreement is achieved with the form of the experimental data points. This equation thus describes very well the fundamental form of the anisotropy vs. Poisson's ratio data in the case of minimum Poisson's ratios as shown in Fig. 4a. Here we have removed the outlying layered materials and also those for which data are measured close to a phase transition, so that $A^* < 35$. In addition, at the limit of $\lambda_1 \to 0$ ($A^* \to 1$) we have isotropy and normal force interaction; here $v \approx 1/4$, the standard point-to-point, Cauchy value for the Poisson's ratio. This analysis suggests that if an atomic interaction in a particular plane is dominated by "sphere-to-sphere" contacts, then these negative extremal Poisson's ratios occur in planes where high structural density is found (whether it be the modulation of cumulative atomic or of electronic density in a particular crystal direction).

Taking this approach further, we propose that extreme positive Poisson's ratios will occur in planes of low structural density and hence that a more appropriate model is a simple atom-to-atom spring model. Such approaches have been used many times, but one of the simplest is described by Feynman [54]. Here, at least two spring constants are required (essential for Poisson's ratio to be anything other than ¼); k_1, nearest neighbour interaction spring constant and k_2, second nearest neighbour interaction spring constant. Feynman's own simple two-dimensional model gives:
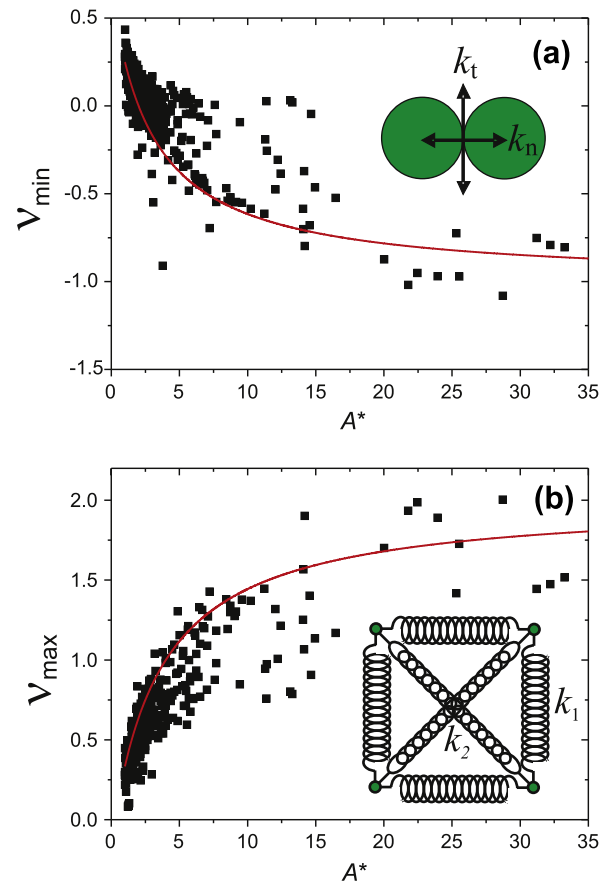

Fig. 4. Simulation of extreme Poisson's ratio vs. A^* curves. In (a) the minimum Poisson's ratio curve has a form that is consistent with a model of close-packed spheres (two of which are shown in the inset) and in (b) the maximum Poisson's ratio curve is simulated by a model of point atoms linked by springs (shown in two dimensions in the inset). Thus the occurrence of extreme values of Poisson's ratio in single-crystalline materials is related to the variation of structural density within their atomic-scale structures.

$$v = (1 + \lambda_2)/(3 + 2\lambda_2) \tag{8}$$

where $\lambda_2 = k_1/k_2$. Plotted in Fig. 4b is the situation for the maximum Poisson's ratio curves where we have used the form:

$$v_{max} = (1 + 4\lambda_2)/(3 + 2\lambda_2) \tag{9}$$

This takes into account that we have moved from two dimensions to three. Here we have defined $\lambda_2 = (A^* - 1)/3$: the use of these constants successfully replicates the general form of the observed points. Hence the two curves used in Fig. 2a and b are very simply related by:

$$\lambda_1 = 3\lambda_2 \tag{10}$$

Eqs. (7) and (9) do not predict the same values for v when $A^* = 1$ ($v_{min} = 0.25$ and $v_{max} = 0.33$), which is not surprising since they are both simple approximate descriptions of the real atomic interactions. These considerations, however, provide a basis for consideration of how real atomic-scale structure dictates bulk elastic properties and by detailed analysis of the crystal structures of each of the materials we

have considered, the simple models could be refined. This will be the subject of future work.

4. Conclusions

A survey of experimental elastic constants of nearly 500 materials shows that many real single crystals possess auxetic behaviour in one or more directions. This is an important observation in understanding structure–property relationships in functional materials. The direction of extreme Poisson's ratio are usually not co-incident with a principal crystallographic axis (i.e., parallel to a unit cell edge) and hence have typically not been noticed or reported with measured elastic constants, since computation on the non-axial properties is non-trivial for the lower symmetry materials. A number of apparently simple materials possess negative Poisson's ratios in certain crystallographic directions, in addition to the metals and alloys previously discussed in the literature: this includes inorganic materials such as the transition-metal oxide ReO_3 and the mineral $CaSO_4$, the elements solid iodine (a molecular material) and the infinite chain structure of trigonal, elemental selenium, and organic solids such as triphenylbenzene and urea. Each of these materials would now be interesting to study in detail to try to link their elastic properties to their atomic-scale structures. This could also lead to a greater understanding of other "unusual" properties of some of these materials: for example, ReO_3 has recently been the focus of attention because of its negative thermal expansion [55].

Although many mathematical analyses have predicted the theoretical bounds of Poisson's ratios for all crystal symmetries, we have used experimentally derived elastic constants. It is interesting to note that while the simple models we propose for the general correlation between elastic anisotropy, extreme Poisson's ratios and atomic-scale structure, are scale-independent, in fact the practically achievable range for most single-crystalline materials appears to be limited by the curves presented in Fig. 4. This is true for a range of materials, whether dominated by largely ionic, covalent or metallic bonding, or indeed for molecular materials, where weaker intermolecular forces are present, such as hydrogen bonds or van der Waals forces.

Appendix A. Supplementary material

Supplementary data associated with this article can be found, in the online version, at doi:10.1016/j.actamat.2010.08.006.

References

[1] Evans KE, Nkansah MA, Hutchinson IJ, Rogers SC. Nature 1991;353:124.
[2] Lakes RS. Adv Mater 1993;5:293.
[3] Alderson A. Chem Ind 1999:384.
[4] Baughman RH. Nature 2003;425:667.
[5] Yang W, Li Z-M, Shi W, Xie B-H, Yang M-B. J Mater Sci 2004;39:3269.
[6] Lakes R. Science 1987;235:1038.
[7] Caddock BD, Evans KE. J Phys D – Appl Phys 1989;22:1877.
[8] Baughman RH, Shacklette JM, Zakhidov AA, Stafstrom S. Nature 1998;392:362.
[9] Yeganeh-Haeri A, Weidner DJ, Parise JB. Science 1992;257:650.
[10] Ogi H, Fukunaga M, Hirao M, Ledbetter H. Phys Rev B 2004;69:024104.
[11] Williams JJ, Smith CW, Evans KE, Lethbridge ZAD, Walton RI. Chem Mater 2007;19:2423.
[12] Grima JN, Jackson R, Alderson A, Evans KE. Adv Mater 2000;12:1912.
[13] Alderson A, Evans KE. Phys Rev Lett 2002;89.
[14] Every AG, McCurdy AK. Landolt-Börnstein numerical data and functional relationships in science and technology, new series, group III: crystal and solid state physics. Low frequency properties of dielectric crystals, subvolume a: second and higher order elastic constants, vol. 29. Springer-Verlag; 1992.
[15] Lempriere BM. J Am Inst Aeronaut Astronaut 1968:2226.
[16] Boulanger P, Hayes M. J Elasticity 1998;50:87.
[17] Rovati M. Scr Mater 2003;48:235.
[18] Rovati M. Scr Mater 2004;51:1087.
[19] Ting TCT, Chen TY. Q J Mech Appl Math 2005;58:73.
[20] Ting TCT, Barnett DM. J Appl Mech – Trans ASME 2005;72:929.
[21] Norris AN. Proc Roy Soc A – Math Phys Eng Sci 2006;462:3385.
[22] Zhang JM, Zhang Y, Xu KW, Ji V. J Phys Chem Solids 2007;68:503.
[23] Zhang JM, Zhang Y, Xu KW, Ji V. Phys B – Condens Matter 2007;390:106.
[24] Paszkiewicz T, Wolski S. Phys Status Solidi B – Basic Solid State Phys 2007;244:966.
[25] Nye JF. Physical properties of crystals: their representation by tensors and matrices. Oxford: Oxford University Press; 1985.
[26] Zener C. Phys Rev 1947;71:846.
[27] Jona F, Marcus PM. J Phys – Condens Matter 2001;13:5507.
[28] Tsuchiya T, Kawamura K. J Chem Phys 2002;116:2121.
[29] Karki BB, Stixrude L, Clark SJ, Warren MC, Ackland GJ. Crain J Am Miner 1997;82:51.
[30] Farajov VD, Iskenderzade ZA, Kasumova EK, Kurbanov EM. Inorg Mater 2005;41:911.
[31] Karki BB, Stixrude L, Crain J. Geophys Res Lett 1997;24:3269.
[32] Turley J, Sines G. J Phys D – Appl Phys 1971;4:264.
[33] Li Y. Phys Status Solidi A – Appl Res 1976;38:171.
[34] Li Y, Chung DY. Phys Status Solidi A – Appl Res 1978;46:603.
[35] Ledbetter H, Migliori A. J Appl Phys 2006:100.
[36] Ranganathan SI, Ostoja-Starzewski M. Phys Rev Lett 2008:101.
[37] Marmier ASH, Lethbridge ZAD, Walton RI, Smith CW, Parker SC, Evans KE. Comp Phys Commun; in press. **Q1**
[38] Arlt G, Schweppe H. Solid State Commun 1968;6:783.
[39] Uchida N, Ohmachi Y. J Appl Phys 1969;40:4692.
[40] Ohmachi Y, Uchida N. J Appl Phys 1970;41:2307.
[41] Ogi H, Fukunaga M, Hirao M, Ledbetter H. Phys Rev B 2004:69.
[42] Feldman JL. J Phys Chem Solids 1976;37:1141.
[43] Gunton DJ, Saunders GA. J Mater Sci 1972;7:1061.
[44] Carpenter MA, Salje EKH. Eur J Miner 1998;10:693.
[45] Errandonea G. Phys Rev B 1980;21:5221.
[46] Gunton DJ, Saunders GA. Proc Roy Soc Lond Ser A – Math Phys Eng Sci 1975;343:63.
[47] Gunton DJ, Saunders GA. Solid State Commun 1974;14:865.
[48] Chung DY, Gunton DJ, Saunders GA. Phys Rev B 1976;13:3239.
[49] Nakanishi N. Prog Mater Sci 1979;24:143.
[50] Haussühl S. Solid State Commun 1988;68:963.
[51] Kushida T, Terhune RW. Phys Rev B 1986;34:5791.
[52] Bathurst RJ, Rothenburg L. Int J Eng Sci 1988;26:373.
[53] Rothenburg L, Berlin AA, Bathurst RJ. Nature 1991;354:470.
[54] Feyman RP, Leighton RB, Sands M. The Feyman lectures on physics, vol II, 38–1 to 39–13. Reading MA Adison Wesley; 1972.
[55] Chatterji T, Henry PF, Mittal R, Chaplot SL. Phys Rev B 2008:78.